Journal of Solid Mechanics Vol. 17, No. 3 (2025) pp. 245-259
DOI: 10.60664/jsm.2025.3061779

Research Paper

The Dynamic Response of Coupling Thermo Mechanical of Sandwich Graphene-Reinforced Titanium-Based Composite Beams with Soft Porous Core (PE Open Cell Foam) Under Two Moving Constant Loads on the Thermal Environment Under Elastic Medium

M.R. Eghbali [1], S.A.H. Hosseini [2*]

[1]*Department of Mechanical Engineering, University of Zanjan, Zanjan, Iran*
[2]*Department of Industrial, Mechanical and Aerospace Engineering, Buin Zahra, Buin Zahra, Iran*

Received 10 June 2023; Received in revised form 5 May 2025; Accepted 12 November 2025

ABSTRACT

Dynamic analysis of sandwich beams is very important in industrial applications, so in this article, the dynamic response of this type of structure is investigated. In this type of structure, functionally graded (FG) reinforcement layers are usually used to improve the mechanical properties of the structure, which is important according to the desired work performance. Therefore, in this paper, the dynamic response of graphene reinforced titanium-based composite (GRTC) sandwich beam with a soft porous core (PE open cell foam) on a Winkler-Pasternak substrate in a thermal environment has been used. The equations are derived using higher-order hyperbolic shear deformation theory in both axial and transverse directions. In the following, using the Laplace method, the problem is solved accurately under two moving loads, which has not been done with this method. The advantages of this method are the simplicity of solving and reducing to zero the error percentage that exists in numerical solutions. The results are compared with previous works and finally, the effect of various parameters such as temperature, porosity coefficient, elastic constant, thickness ratio and velocity of moving load on the dynamic response of the sandwich beam is investigated. It should be noted that the results can be used in the construction of this type of structure.

Keywords: GRTC sandwich beams*;* Moving load*;* Porous materials*;* Elastic foundation*;* Exact solution*;* Thermal environment.

1 INTRODUCTION

SANDWICH structures are often used in weight-sensitive industries such as automotive, aircraft and marine

*Corresponding author. Tel.: +98 9127839315.
E-mail address: hosseini@znu.ac.ir (S.A.H. Hosseini)

equipment [1]. A sandwich beam consists of two thin, strong and rigid facets that are glued on both sides to a thick, light and weak core. The role of the core is as a support to prevent shear failure of the facets. Core building materials can usually include foams, corrugated sheets, honeycomb sheets, and balsa wood. In contrast, face sheets increase the strength of the sandwich structure. Their material can be metallic and non-metallic; the steel and aluminum materials used in facets are of metal type. Also, fiber-reinforced composites are of non-metallic type, which is made in facets. It can be used.

In studying the vibrations of sandwich beams, it is especially important to know the type of displacement fields of the beam. Various theories have been used for displacement fields. For example, first-order shear deformation theory [2] and higher-order shear deformation theories [3-6] have been used to study the vibrational behavior of sandwich beams. Kapuria et al. Also used zigzag theories to express the displacement fields of sandwich beams. Using this theory, they studied the vibrations of sandwich beams and stated that the use of zigzag theories has increased the accuracy in calculating the natural frequency [7, 8].

Dynamic modeling of sandwich structures is found in abundance. Meanwhile, Moreira and Rodrigues investigated the static and dynamic behavior of sandwich plates and beams using the LayerWise model. They showed that the proposed model has good accuracy for a high modulus ratio [9]. Vidal and Polit investigated the free vibrations of multilayer beams using the finite element method. They used a three-point element with a Sine distribution [10]. Khalili et al. Investigated the vibrations of sandwich beams using dynamic stiffness and finite element methods [11]. Hwu et al. Investigated the free and forced vibrations of sandwich beams by considering transverse shear and rotational inertial deformation [12]. Lou and colleagues examined the free vibration of sandwich beams by considering the pyramidal truss core. They obtained the natural frequency of the system by constantly considering the thickness of the beam [13]. Piollet et al. Investigated the nonlinear vibrations of sandwich beams by considering entangled cross-linked fiber (ECF) material. The effect of ECF increased the damping of the structure. They also examined the frequency response of the beam for various parameters such as dumping [14].
Huang et al. Examined the free vibrations of the sandwich beam by considering the properties of the core viscoelastic. They investigated the effect of stiffness and damping of viscoelastic nuclei on natural frequency [15]. Rokn-Abadi et al. Examined the free vibrations of sandwich beams in the presence of magnetoelastic loads. They investigated the effect of the magnetic field on the natural frequency of the beam [16]. Souza Eloy et al. Numerically and practically studied the vibrations of the sandwich beam by considering the magnetic elastomeric honeycomb core [17]. Wang and Zhao investigated the free vibrations of sandwich beams using the Chebyshev collocation method. The core of the sandwich beam is made of foam metal [18]. Fadaee proposed an accurate method for analyzing the damped vibration of magnetorheological fluid (MRF) sandwich beams based on the Tymoshenko beam model. Thickness changes in MRF cause severe changes in normal frequency [19]. Wang and Shen investigated the nonlinear vibrations of sandwich plates in a thermal environment. The considered sheets are graphene-reinforced composites [20].

Jin et al. Studied the nonlinear vibrations of post-buckling sandwich beams with the zigzag theory of higher-order shear deformation theory. They have used graphene reinforced composites in face sheets. Using the improved Lindstead Poincaré method, the frequency response of the sandwich beam was calculated [21]. Singha et al. Examined the free vibrations of a rotating pre-twisted sandwich conical shell in the presence of temperature. Using the finite element method and the theory of higher-order shear deformation theory, they obtained the natural frequency of the sandwich beam and investigated the effect of the graphene-reinforced composite on the face sheets [22]. Shen and Fan investigated the nonlinear vibrations of graphene-reinforced (GRC) composite laminates in a thermal environment. FG Graphene-reinforced layers are considered in the direction of thickness [23]. Mohammadi and Nematollahi investigated the forced vibrations of composite beams reinforced with graphene platelets. FG Graphene platelets-reinforced face sheets are considered. Using the theory of high-order shear deformation theory, the governing equations of extraction and natural frequency were investigated under different conditions [24].

Due to the importance of dynamic loads on sandwich structures, in this paper, the dynamic response of sandwich beams reinforced with a graphene layer of metal base (Titanium) with a porous softcore (PE open cell foam) on a Winkler-Pasternak substrate in a thermal environment is investigated. Assuming displacement fields according to hyperbolic higher-order shear deformation theory, the governing equations of vibration were obtained in both transverse and longitudinal directions. Then, using the Laplace method, the dynamic response of the sandwich beam was obtained. In the results section, the effect of various parameters such as temperature, porosity coefficient, thickness ratio and velocity of moving load on the dynamic response of the system is investigated.

2 FORMULATION OF THE PROBLEM

A schematic of the functionally graded (FG) graphene reinforced titanium-based composite (GRTC) sandwich beam under thermal load is shown in Fig. 1. These geometrical parameters of length L, width is w, thicknesses h_t, h_c and h_b are referred to the top, core, and bottom layers, respectively; therefore, thickness is $h = h_t + h_c + h_b$. Also, the sandwich beam is supposed to have a porous core and two graphenes reinforced titanium-based composite face sheets.

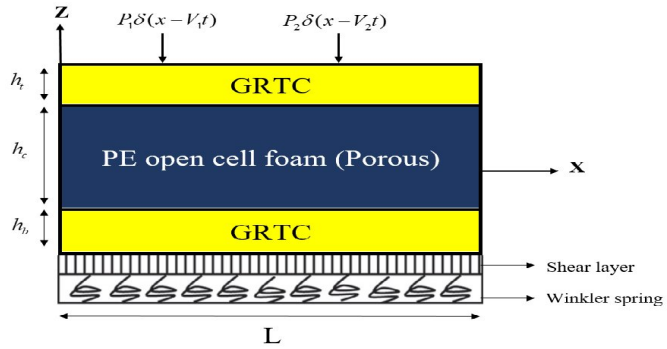

Fig. 1
A schematic diagram of the considering sandwich beam.

2.1 Porous core

This paper uses a softcore (PE open cell foam). Also, asymmetric porosity of the core is considered. Fig. 1 mechanical properties of the porous core can be estimated as three different functions as follow [25]:
Symmetric:

$$E(z) = E_1(1 - e_0 \cos(\frac{\pi z}{h_c}))$$
$$\rho(z) = \rho_1(1 - e_m \cos(\frac{\pi z}{h_c})) \quad (1)$$

Asymmetric:

$$E(z) = E_1(1 - e_0 \cos(\frac{\pi z}{h_c} + \frac{\pi}{4}))$$
$$\rho(z) = \rho_1(1 - e_m \cos(\frac{\pi z}{h_c} + \frac{\pi}{4})) \quad (2)$$

Uniform:

$$E(z) = E_1(1 - e_0 a)$$
$$\rho(z) = \rho_1\sqrt{1 - e_0 a} \quad (3)$$

where [25]:

$$a = \frac{1}{e_0} - \frac{1}{e_0}(\frac{2}{\pi}\sqrt{1 - e_0 a} - \frac{2}{\pi} + 1)^2 \quad (4)$$

In which E_1, ρ_1 and E_2, ρ_2 indicate the maximum and minimum values of Young's elasticity modulus and density, respectively. Also e_0 and e_m are the coefficients of porosity and mass density. Using the Eqs. **Error! Reference source not found.-Error! Reference source not found.** the relationship between e_0 and e_m can be obtained as [25]:

$$e_m = 1 - \sqrt{1 - e_0} \tag{5}$$

2.2 U-GRTC face sheets

Today, the use of graphene in the industry is increasing. Applications of graphene include electronic applications, electronics applications, applications in the manufacture of composites for reinforcement, medical engineering, energy storage, the manufacture of transistors, and the production of super batteries. Therefore, the study of this article of research is of great importance [26].

In this study, graphene was used as a face for reinforcement. Among the various modes of graphene, the U-GRTC is used in this paper $V_{GRT} = V_{GRT}^*$. The total volume fraction of GRT (V_{GRT}^*) like as below [27]:

$$V_{GRT}^* = \frac{O_{GRT}}{O_{GRT} + (\frac{\rho_{GRT}}{\rho_{Ti}})(1 - O_{GRT})} \tag{6}$$

where is GRT weight fraction, and are the mass densities of GRTs and the polymer matrix, respectively. The elastic modulus of composites like as below [27]:

$$E = E_{Ti}[\frac{3(1 + \xi_L \eta_L V_{GRT})}{8(1 - \eta_L V_{GRT})} + \frac{5(1 + \xi_W \eta_W V_W)}{8(1 - \eta_W V_W)}] \tag{7}$$

where:

$$\eta_L = \frac{(\frac{E_{GRT}}{E_{Ti}}) - 1}{(\frac{E_{GRT}}{E_{Ti}}) + \xi_L},\ \eta_W = \frac{(\frac{E_{GRT}}{E_{Ti}}) - 1}{(\frac{E_{GRT}}{E_{Ti}}) + \xi_W},\ \xi_L = 2(\frac{L_{GRT}}{h_{GRT}}),\quad \xi_L = 2(\frac{W_{GRT}}{h_{GRT}}) \tag{8}$$

where in Eq. **Error! Reference source not found.** E_{Ti} is Young's modulus of the Titanium and $E_{GRT}, L_{GRT}, W_{GRT}, h_{GRT}$ are the Young's modulus, length, width and thickness of GRT. Also $h_{GRT} = h_t = h_b$.

Poisson's ratios, densities and thermal expansion coefficients of the face sheets like as below [27]:

$$\begin{aligned} \upsilon &= \upsilon_{GRT} V_{GRT} + \upsilon_{Ti}(1 - V_{GRT}) \\ \rho &= \rho_{GRT} V_{GRT} + \rho_{Ti}(1 - V_{GRT}) \\ \alpha &= \alpha_{GRT} V_{GRT} + \alpha_{Ti}(1 - V_{GRT}) \end{aligned} \tag{9}$$

3 GOVERNING EQUATIONS

The shear deformation beam theory the axial and transverse displacement field can be expressed as follows [28]:

$$u(x,z,t) = u_0 - z\frac{\partial w_0(x,t)}{\partial x} + \Psi(z) f_0(x,t) \tag{10}$$
$$w(x,z,t) = w_0(x,t)$$

where u_0 and w_0 are the axial and transverse displacement, respectively $\Psi(z)$, shape function. f_0 and $\Psi(z)$, defined as the transverse shear strain, can be expressed as [28]:

$$f_0(x,t) = \frac{\partial w_0(x,t)}{\partial x} - \phi_0(x,t) \tag{11}$$
$$\Psi(z) = h\sinh(\frac{z}{h}) - z\cosh(0.5)$$

where ϕ_0 is the total bending rotation of the cross-section, and t is time. The expression of normal and shear strain components associated with the displacement field in Eq. **Error! Reference source not found.** follows.

$$\varepsilon_{xx} = \frac{\partial u_0}{\partial x} - z\frac{\partial^2 w_0}{\partial x^2} + \Psi(z)(\frac{\partial^2 w_0}{\partial x^2} - \frac{\partial \phi_0}{\partial x}) \tag{12}$$

$$\gamma_{xz} = \frac{\partial \Psi(z)}{\partial z}(\frac{\partial w_0}{\partial x} - \phi_0) \tag{13}$$

where:

$$\begin{aligned}&\frac{dN_x}{dx} = I_0\ddot{u}_0 - I_1\frac{d\ddot{w}_0}{dx} + I_3(\frac{d\ddot{w}_0}{dx} - \ddot{\phi}_0)\frac{d^2P_x}{dx^2} - \frac{d^2M_x}{dx^2} + \frac{dQ_x}{dx} - f + k_w w_0 - k_s\frac{d^2w_0}{dx^2} - N_{x0}\frac{d^2w_0}{dx^2} = I_0\ddot{w}_0 - I_1\frac{d\ddot{u}_0}{dx} + \\ &I_2\frac{d^2\ddot{w}_0}{dx^2} + I_3\frac{d\ddot{u}_0}{dx} + I_4(\frac{d\ddot{\phi}_0}{dx} - 2\frac{d^2\ddot{w}_0}{dx^2}) + I_5(\frac{d^2\ddot{w}_0}{dx^2} - \frac{d\ddot{\phi}_0}{dx}) - \frac{dP_x}{dx} - Q_x = -I_3\ddot{u}_0 + I_4\frac{d\ddot{w}_0}{dx} - I_5(\frac{d\ddot{w}_0}{dx} - \ddot{\phi}_0)\end{aligned} \tag{14}$$

where N_x, M_x, P_x and Q_x are the stress resultants in terms of the normal force, bending moment, higher-order generalized force, and shear force, respectively.

$$N_x = A_{11}\frac{du_0}{dx} - B_{11}\frac{d^2w_0}{dx^2} + C_{11}(\frac{d^2w_0}{dx^2} - \frac{d\phi_0}{dx}) \tag{15}$$

$$M_x = B_{11}\frac{du_0}{dx} - D_{11}\frac{d^2w_0}{dx^2} + E_{11}(\frac{d^2w_0}{dx^2} - \frac{d\phi_0}{dx}) \tag{16}$$

$$P_x = C_{11}\frac{du_0}{dx} - E_{11}\frac{d^2w_0}{dx^2} + H_{11}(\frac{d^2w_0}{dx^2} - \frac{d\phi_0}{dx}) \tag{17}$$

$$Q_x = A_{55}(\frac{dw_0}{dx} - \phi_0) \tag{18}$$

In Eq. **Error! Reference source not found.** to Eq., **Error! Reference source not found.** we have:

$$[A_{11}, B_{11}, D_{11}] = \int_{-\frac{hc}{2}-h_b}^{-\frac{hc}{2}} Q_{11}^b[1, z, z^2]dz + \int_{-\frac{hc}{2}}^{\frac{hc}{2}} A(z)[1, z, z^2]dz + \int_{\frac{hc}{2}}^{\frac{hc}{2}+h_t} Q_{11}^t[1, z, z^2]dz \tag{19}$$

$$[C_{11}, E_{11}] = \int_{-\frac{hc}{2}-h_b}^{-\frac{hc}{2}} Q_{11}^b\Psi(z)[1, z]dz + \int_{-\frac{hc}{2}}^{\frac{hc}{2}} A(z)\Psi(z)[1, z]dz + \int_{\frac{hc}{2}}^{\frac{hc}{2}+h_t} Q_{11}^t\Psi(z)[1, z]dz \tag{20}$$

$$H_{11}=\int_{-\frac{hc}{2}-h_b}^{-\frac{hc}{2}} Q_{11}^{b}\Psi^{2}(z)dz+\int_{-\frac{hc}{2}}^{\frac{hc}{2}} A(z)\Psi^{2}(z)dz+\int_{\frac{hc}{2}}^{\frac{hc}{2}+h_t} Q_{11}^{t}\Psi^{2}(z)dz \tag{21}$$

$$A_{55}=\int_{-\frac{hc}{2}-h_b}^{-\frac{hc}{2}} Q_{55}^{b}(\frac{d\Psi(z)}{dz})^{2}dz+\int_{-\frac{hc}{2}}^{\frac{hc}{2}} G(z)(\frac{d\Psi(z)}{dz})^{2}dz+\int_{\frac{hc}{2}}^{\frac{hc}{2}+h_t} Q_{55}^{t}(\frac{d\Psi(z)}{dz})^{2}dz \tag{22}$$

where the superposed dot on a variable indicates time derivative and I_i *(i* = 0,1,2...5*)* are the mass moments of inertia defined as:

$$[I_0,I_1,I_2]=\int_{-\frac{hc}{2}-h_b}^{-\frac{hc}{2}} \rho^{b}[1,z,z^{2}]dz+\int_{-\frac{hc}{2}}^{\frac{hc}{2}} \rho(z)[1,z,z^{2}]dz+\int_{\frac{hc}{2}}^{\frac{hc}{2}+h_t} \rho^{t}[1,z,z^{2}]dz \tag{23}$$

$$[I_3,I_4]=\int_{-\frac{hc}{2}-h_b}^{-\frac{hc}{2}} \rho^{b}\Psi(z)[1,z]dz+\int_{-\frac{hc}{2}}^{\frac{hc}{2}} \rho(z)\Psi(z)[1,z]dz+\int_{\frac{hc}{2}}^{\frac{hc}{2}+h_t} \rho^{t}\Psi(z)[1,z]dz \tag{24}$$

$$I_5=\int_{-\frac{hc}{2}-h_b}^{-\frac{hc}{2}} \rho^{b}\Psi^{2}(z)dz+\int_{-\frac{hc}{2}}^{\frac{hc}{2}} \rho(z)\Psi^{2}(z)dz+\int_{\frac{hc}{2}}^{\frac{hc}{2}+h_t} \rho^{t}\Psi^{2}(z)dz \tag{25}$$

Also, in Eq. **Error! Reference source not found.** we have:

$$\begin{aligned} &k_w=\frac{\beta_w A_{110}}{L^{2}},\ k_s=\beta_s A_{110}\\ &N_{x0}=\int_{-\frac{hc}{2}-h_b}^{-\frac{hc}{2}} E_{11}^{b}\alpha^{b}\,\Delta T\,dz+\int_{-\frac{hc}{2}}^{\frac{hc}{2}} E(z)\alpha(z)\,\Delta T\,dz+\int_{\frac{hc}{2}}^{\frac{hc}{2}+h_t} E_{11}^{t}\alpha^{t}\,\Delta T\,dz \end{aligned} \tag{26}$$

K_w and k_s are the Winkler and shearing layer spring constants. β_w and β_s are the corresponding spring constant factors. It is also defined that A_{110} is the value of A_{11} of a homogeneous beam.

The stress resultants of Eqs. **Error! Reference source not found.-Error! Reference source not found.** are substituted into Eq. **Error! Reference source not found.** to obtain the equations of motion or the governing equations in the form of displacements as follows:

$$A_{11}\frac{d^{2}u_0}{dx^{2}}-B_{11}\frac{d^{3}w_0}{dx^{3}}+C_{11}(\frac{d^{3}w_0}{dx^{3}}-\frac{d^{2}\phi_0}{dx^{2}})=I_0\ddot{u}_0-I_1\frac{d\ddot{w}_0}{dx}+I_3(\frac{d\ddot{w}_0}{dx}-\ddot{\phi}_0) \tag{27}$$

$$\begin{aligned} &C_{11}\frac{d^{3}u_0}{dx^{3}}-E_{11}\frac{d^{4}w_0}{dx^{4}}+H_{11}(\frac{d^{4}w_0}{dx^{4}}-\frac{d^{3}\phi_0}{dx^{3}})-B_{11}\frac{d^{3}u_0}{dx^{3}}+D_{11}\frac{d^{4}w_0}{dx^{4}}-E_{11}(\frac{d^{4}w_0}{dx^{4}}-\frac{d^{3}\phi_0}{dx^{3}})+A_{55}(\frac{d^{2}w_0}{dx^{2}}-\frac{d\phi_0}{dx})\\ &-f+k_w w_0-k_s\frac{d^{2}w_0}{dx^{2}}-N_{x0}\frac{d^{2}w_0}{dx^{2}}=I_0\ddot{w}_0-I_1\frac{d\ddot{u}_0}{dx}+I_2\frac{d^{2}\ddot{w}_0}{dx^{2}}+I_3\frac{d\ddot{u}_0}{dx}+I_4(\frac{d\ddot{\phi}_0}{dx}-2\frac{d^{2}\ddot{w}_0}{dx^{2}})+I_5(\frac{d^{2}\ddot{w}_0}{dx^{2}}-\frac{d\ddot{\phi}_0}{dx}) \end{aligned} \tag{28}$$

$$-C_{11}\frac{d^{2}u_0}{dx^{2}}+E_{11}\frac{d^{3}w_0}{dx^{3}}-H_{11}(\frac{d^{3}w_0}{dx^{3}}-\frac{d^{2}\phi_0}{dx^{2}})-A_{55}(\frac{dw_0}{dx}-\phi_0)=-I_3\ddot{u}_0+I_4\frac{d\ddot{w}_0}{dx}-I_5(\frac{d\ddot{w}_0}{dx}-\ddot{\phi}_0) \tag{29}$$

4 ANALYTICAL SOLUTION

The assumed mode method is utilized for the discretization of the unknown fields of the problem in the spatial domain. Therefore [29]:

$$u_0(x,t)=\sum_{n=1}^{\infty}U_n(t)\cos(\frac{n\pi x}{L}) \tag{30}$$

$$w_0(x,t)=\sum_{n=1}^{\infty}W_n(t)\sin(\frac{n\pi x}{L}) \tag{31}$$

$$\phi_0(x,t)=\sum_{n=1}^{\infty}\Phi_n(t)\cos(\frac{n\pi x}{L}) \tag{32}$$

$U_n(t),W_n(t)$ and $\Phi_n(t)$ are the unknown Fourier coefficients to be determined for each *n* value. By using the general property of Dirac Delta function as follows [29]:

$$\begin{aligned}&\delta(x-V_1t)=2\sum_{n=1}^{\infty}\sin(\frac{n\pi x}{L})\sin(\frac{n\pi V_1t}{L})\\&\delta(x-V_2t)=2\sum_{n=1}^{\infty}\sin(\frac{n\pi x}{L})\sin(\frac{n\pi V_2t}{L})\\&\alpha=(\frac{n\pi}{L})\end{aligned} \tag{33}$$

with the initial condition:

$$W_n(0)=\dot{W}_n(0)=U_n(0)=\dot{U}_n(0)=\Phi_n(0)=\dot{\Phi}_n(0)=0 \tag{34}$$

The continuation of the solution is with Laplace making, the relations of which are given below as a reminder:

$$\begin{aligned}&L\left[\ddot{W}_n(t)\right]=s^2W_n(s)-sW_n(0)-\dot{W}_n(0),\quad W_n(s)=L[W_n(t)]\\&L\left[\ddot{U}_n(t)\right]=s^2U_n(s)-sU_n(0)-\dot{U}_n(0),\quad U_n(s)=L[U_n(t)]\\&L\left[\ddot{\Phi}_n(t)\right]=s^2\Phi_n(s)-s\Phi_n(0)-\dot{\Phi}_n(0),\quad \Phi_n(s)=L[\Phi_n(t)]\end{aligned} \tag{35}$$

By placing Eqs. **Error! Reference source not found.-Error! Reference source not found.** in Eqs. **Error! Reference source not found.-Error! Reference source not found.**, and we get Laplace:

$$\begin{pmatrix}K_{11}&K_{12}&K_{13}\\K_{12}&K_{22}&K_{23}\\K_{13}&K_{23}&K_{33}\end{pmatrix}\begin{Bmatrix}U_n(s)\\W_n(s)\\\Phi_n(s)\end{Bmatrix}=\begin{Bmatrix}0\\F\\0\end{Bmatrix} \tag{36}$$

where:

$$\begin{aligned}&K_{11}=-A_{11}\alpha^2-I_0s^2,\quad K_{12}=B_{11}\alpha^3-C_{11}\alpha^3+I_1\alpha s^2-I_3\alpha s^2,\quad K_{13}=C_{11}\alpha^2+I_3s^2\\&K_{22}=2E_{11}\alpha^4-H_{11}\alpha^4-D_{11}\alpha^4+A_{55}\alpha^2+k_w+k_s\alpha^2-N_{x0}\alpha^2+I_0s^2-I_2\alpha^2s^2+2I_4\alpha^2s^2-I_5\alpha^2s^2\\&K_{23}=+H_{11}\alpha^3-E_{11}\alpha^3-A_{55}\alpha-I_4\alpha s^2+I_5\alpha s^2,\quad K_{33}=-H_{11}\alpha^2+A_{55}-I_5s^2\\&F=\frac{2P_1(\alpha V_1)}{s^2+(\alpha V_1)^2}+\frac{2P_2(\alpha V_2)}{s^2+(\alpha V_2)^2}\end{aligned} \tag{37}$$

By applying in inverse Laplace transform to Eq. **Error! Reference source not found.**, the transverse and axial dynamic response of sandwich beam is obtained:

$$U_n(x,t)=\frac{1}{y_2}\left(\frac{y_1\sin\left[\sqrt{d_{18}}\,t\right]}{\sqrt{d_{18}}}\right)+\frac{1}{y_4}\left(\frac{y_3\sin\left[\sqrt{d_{20}}\,t\right]}{\sqrt{d_{20}}}\right)+\frac{\left(Z_1\sinh\left[t\sqrt{x_1}\right]+Z_2\sinh\left[t\sqrt{x_2}\right]+Z_3\sinh\left[t\sqrt{x_3}\right]\right)}{\det(k)} \tag{38}$$

$$W_n(x,t)=\frac{1}{y_2}\left(\frac{y_5\sin\left[\sqrt{d_{18}}\,t\right]}{\sqrt{d_{18}}}\right)+\frac{1}{y_4}\left(\frac{y_6\sin\left[\sqrt{d_{20}}\,t\right]}{\sqrt{d_{20}}}\right)+\frac{\left(Z_4\sinh\left[t\sqrt{x_1}\right]+Z_5\sinh\left[t\sqrt{x_2}\right]+Z_6\sinh\left[t\sqrt{x_3}\right]\right)}{\det(k)} \tag{39}$$

$$\Phi_n(x,t)=\frac{1}{y_2}\left(\frac{y_7\sin\left[\sqrt{d_{18}}\,t\right]}{\sqrt{d_{18}}}\right)+\frac{1}{y_4}\left(\frac{y_8\sin\left[\sqrt{d_{20}}\,t\right]}{\sqrt{d_{20}}}\right)+\frac{\left(Z_7\sinh\left[t\sqrt{x_1}\right]+Z_8\sinh\left[t\sqrt{x_2}\right]+Z_9\sinh\left[t\sqrt{x_3}\right]\right)}{\det(k)} \tag{40}$$

5 ANALYTICAL RESULTS AND DISCUSSIONS

In this paper, the dynamic response of the sandwich beam on the Winkler-Pasternak foundation is investigated, and metal base (Titanium) graphene was used in this work. In this work, an FG soft porous core is used. Relationships were defined using hyperbolic higher-order shear deformation theory. Taken from Laplace equations and the dynamic response in Laplace space is defined, and finally, with Laplace inversion, the equations in space-time are defined, which is the exact response for the GRT sandwich beam. Finally, the effect of parameters such as spring constants, thickness ratio, speed ratio, moving load speed and temperature was investigated.

In order to check the validity, we intend to evaluate the frequency values with Wu et al. [30]. The relations described in Eq. (38) are performed to calculate dimensionless natural frequencies.

$$\bar{\omega}=\lambda\frac{L^2}{h}\sqrt{\frac{\rho_1}{E_1}} \tag{41}$$

Frequency values were compared and a good validity in terms of frequency values was observed with the reference results. The results are compared with Wu et al. [30] given in Table 1. Also, the dimensions of the beam are: $\frac{L}{h_c}=50,\ L=100,\ h_{GRT}=\frac{h_c}{6},\ w_{GRT}=1$.

Table 1
Comparing the results with previous papers for sandwich beam.

Reference	Mode 1	Mode 2	Mode 3
[30] $V_{CN}^{*}=0.12$	0.1432	0.5650	1.2429
Present	0.1426	0.5640	1.2413
[30] $V_{CN}^{*}=0.17$	0.1560	0.6140	1.3465
Present	0.1556	0.6132	1.3462
[30] $V_{CN}^{*}=0.28$	0.17785	0.6997	1.5246
Present	0.1765	0.6979	1.5231

The effective material properties of GRTC beams and softcore used throughout this paper are given as follows. Matrix material properties are: $\upsilon^{Ti}=0.265,\ \rho^{Ti}=4506\frac{\mathrm{Kg}}{\mathrm{m}^3},\ E^{Ti}=116\,\mathrm{GPa},\ \alpha^{Ti}=1.56\times10^{-6}(K^{-1})$ for reinforcement material $\upsilon_{GRT}=0.186,\ \rho_{GRT}=1060\frac{\mathrm{Kg}}{\mathrm{m}^3},\ E_{GRT}=1.1\mathrm{TPa},\ \alpha_{GRT}=2.35\times10^{-5}(K^{-1})$ and core material $\upsilon_c=0,\ \rho_1=27\ \frac{\mathrm{Kg}}{\mathrm{m}^3}$,

$E_1 = 0.56(MPa)$, $\alpha = 0.038\times10^{-6}(K^{-1})$ [27, 31, 32].

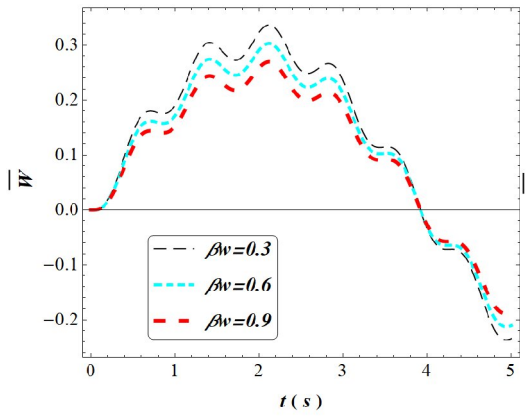

(a) $V_1 = V_2 = 20,\ O_{GRT} = 0.3\%, h_c = \frac{L}{50},$
$h_t = h_b = \frac{h_c}{6}, e_0 = 0.2, \Delta T = 70, \beta_s = 0.02$

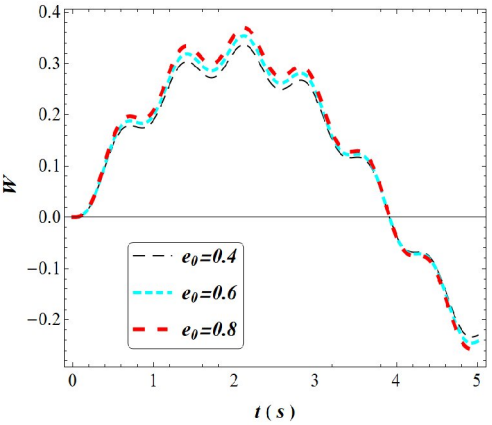

(b) $V_1 = V_2 = 20,\ O_{GRT} = 0.3\%, h_c = \frac{L}{50},$
$h_t = h_b = \frac{h_c}{6}, \beta_w = 0.1, \Delta T = 70, \beta_s = 0.02$

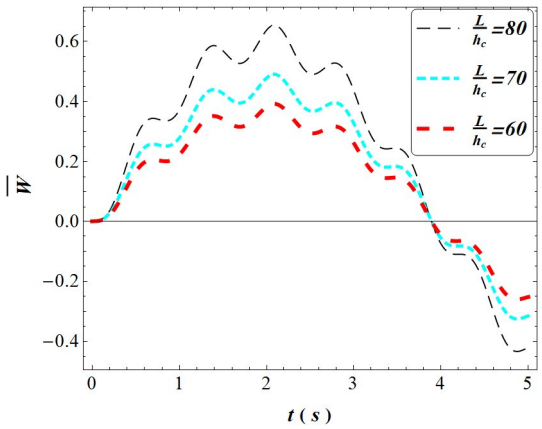

(c) $V_1 = V_2 = 20,\ O_{GRT} = 0.3\%, e_0 = 0.2,$
$h_t = h_b = \frac{h_c}{6}, \beta_w = 0.1, \Delta T = 70, \beta_s = 0.02$

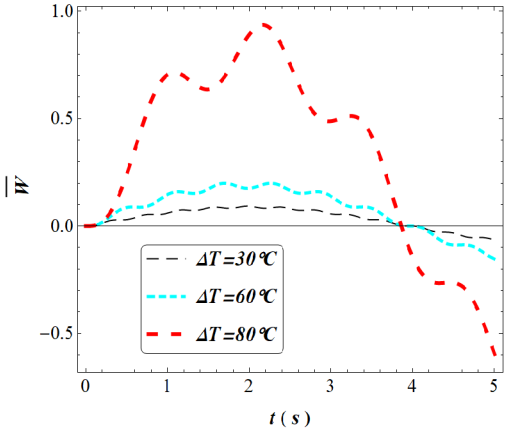

(d) $V_1 = V_2 = 20,\ O_{GRT} = 0.3\%, h_c = \frac{L}{50},$
$h_t = h_b = \frac{h_c}{6}, \beta_w = 0.1, e_0 = 0.2, \beta_s = 0.02$

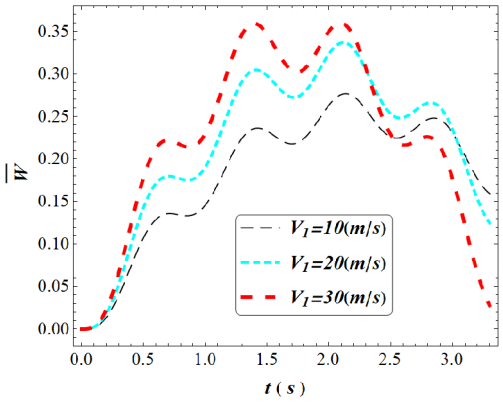

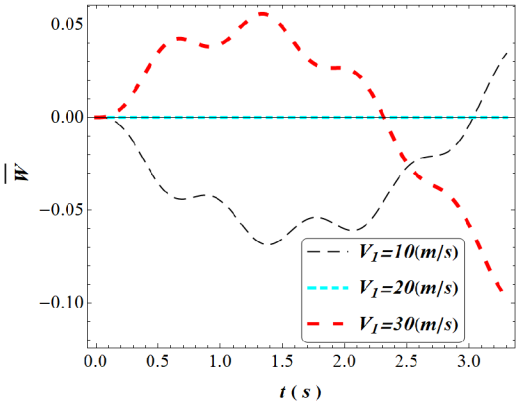

(e) $e_0 = 0.2,\ O_{GRT} = 0.3\%, h_c = \frac{L}{50}, h_t = h_b = \frac{h_c}{6},$
$\beta_w = 0.1, \Delta T = 70, \beta_s = 0.02, P_1 = P_2$

(f) $e_0 = 0.2,\ O_{GRT} = 0.3\%, h_c = \frac{L}{50}, h_t = h_b = \frac{h_c}{6},$
$\beta_w = 0.1, \Delta T = 70, \beta_s = 0.02, P_1 = -P_2$

Fig. 2
Variation of dimensionless transverse dynamic sandwich beam versus time of moving load.

In Figs. 2(a)-(f), variation of dimensionless transverse dynamic deflection of the sandwich beam versus time of moving load on an elastic foundation for the different spring constant, coefficient of porous, thicknesses ratio, temperature and velocity of moving load is shown.

In Fig 2(a), transverse displacement decreases with increasing elastic foundation coefficient. In fact, by increasing the elastic foundation, the sandwich beam acts as a shock absorber and the displacement is reduced.

In Fig 2(b), transverse displacement increases with increasing porosity coefficient. As the porosity coefficient increases, the core of the sandwich beam becomes weaker and less resistant to external forces, and displacement increases.

In Fig 2(c), transverse displacement increases with increasing thickness ratio. As the thickness ratio increases, the sandwich beam becomes thinner and the displacement increases with the application of external forces.

In Fig 2(d), temperature increases, the transverse displacement increases. In fact, increasing the temperature increases the axial force due to increased displacement.

In Fig. 2(e)-(f), in general, when both forces are applied in the same direction, the transverse displacement increases with increasing velocity because as the velocity increases, the external force reaches the center of the beam sooner and the displacement increases.

But when external forces are in the opposite direction, the transverse displacement of the GRTC sandwich beam in the direction of the force is faster. When both velocities are equal, the transverse displacement is zero.

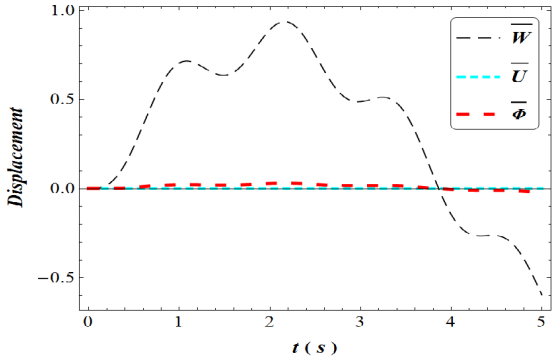

Fig. 3
Variations of dimensionless dynamic deflection a sandwich beam (U-GRTC) versus time of moving load
$V_1 = V_2 = 20,\ O_{GRT} = 0.3\%, h_c = \frac{L}{50}, h_t = h_b = \frac{h_c}{6}, \beta_w = 0.1, \Delta T = 80, \beta_s = 0.02, e_0 = 0.2$.

In Fig. 3, transverse displacement, axial displacement and total banding are shown. As can be seen, the effect of external force is more focused on transverse displacement, which is due to the application of force in this direction. We also have a small amount of total banding and axial displacement. The amount of total banding is slightly more than the transverse displacement.

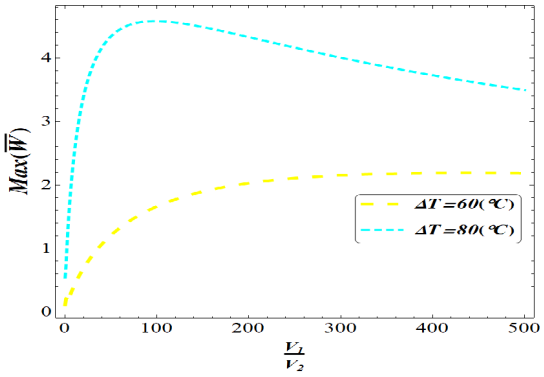

Fig. 4
Maximum dimensionless transverse dynamic displacements of the sandwich beam (U-GRTC) under moving load versus velocity ratio for different temperature $e_0 = 0.2,\ O_{GRT} = 0.3\%, h_c = \frac{L}{50}, h_t = h_b = \frac{h_c}{6}, \beta_w = 0.1, \beta_s = 0.02$.

In Fig. 4, maximum dimensionless transverse dynamic displacements of the sandwich beam under moving load versus velocity ratio for the different temperatures are shown. With increasing temperature, the maximum transverse displacement increases due to considering the effects of temperature in the form of axial force; with increasing temperature, the axial force increases and the displacement increases. Also, with increasing speed ratio, the maximum transverse displacement of the sandwich beam increases.

6 CONCLUSIONS

In this paper, the dynamic response of the sandwich beam on the Winkler-Pasternak foundation is investigated, and metal base (Titanium) graphene was used in this work. In this work, an FG soft porous core is used. Relationships were defined using hyperbolic higher-order shear deformation theory. Taken from Laplace equations and the dynamic response in Laplace space is defined, and finally, with Laplace inversion, the equations in space-time are defined, which is the exact response for the GRT sandwich beam. Finally, the effect of parameters such as spring constants, thickness ratio, speed ratio, moving load speed and temperature was investigated.

As the thickness ratio increases and the moving load velocity increase, the axial and transverse displacement increase. In fact, by increasing the thickness ratio, the beam becomes thinner and less resistant to external forces, and the displacement increases. When the velocity increases, the external force reaches the center of the beam sooner and the displacement increases.

Transverse displacement decreases with a constant spring increase. By increasing the elastic foundation, the GRAC sandwich beam acts as a shock absorber and the displacement is reduced.

Transverse displacement increases with increasing porosity coefficient. As the porosity coefficient increases, the soft core of the sandwich beam becomes weaker and less resistant to external forces, and displacement increases. Also, increasing the temperature increases the axial force due to increased displacement.

APPENDIX A

$$u_1 = 1, \qquad u_2 = \frac{-1 + I\sqrt{3}}{2}, \qquad u_3 = \frac{-1 - I\sqrt{3}}{2}$$

$$\Delta_0 = {g_4}^2 - 3g_6 g_2, \quad \Delta_1 = 2{g_4}^3 - 9g_6 g_4 g_2 + 27{g_6}^2 g_0, \quad Ci = \sqrt[3]{\frac{\Delta_1 + \sqrt{{\Delta_1}^2 - 4{\Delta_0}^3}}{2}}$$

$$x_1 = \frac{-1}{3g_6}\left(g_4 + u_1 Ci + \frac{\Delta_0}{u_1 Ci}\right), \qquad x_2 = \frac{-1}{3g_6}\left(g_4 + u_2 Ci + \frac{\Delta_0}{u_2 Ci}\right), \qquad x_3 = \frac{-1}{3g_6}\left(g_4 + u_3 Ci + \frac{\Delta_0}{u_3 Ci}\right)$$

$$\det(k) = \sqrt{x_1}\sqrt{x_2}\sqrt{x_3}\left(g_2 g_4 - 3g_0 g_6 + 2{g_6}^2\left(x_1 {x_2}^2 + {x_1}^2 x_3 + x_2 {x_3}^2\right)\right)$$

$$\begin{aligned}
Z_1 &= -g_6\left(f_0 + x_1\left(f_2 + f_4 x_1\right)\right)\sqrt{x_2}\left(x_2 - x_3\right)\sqrt{x_3} \\
Z_2 &= g_6\sqrt{x_1}\left(f_0 + x_2\left(f_2 + f_4 x_2\right)\right)\left(x_1 - x_3\right)\sqrt{x_3} \\
Z_3 &= g_6\sqrt{x_1}\sqrt{x_2}\left(-x_1 + x_2\right)\left(f_0 + x_3\left(f_2 + f_4 x_3\right)\right) \\
Z_4 &= -g_6\left(J_0 + x_1\left(J_2 + J_4 x_1\right)\right)\sqrt{x_2}\left(x_2 - x_3\right)\sqrt{x_3} \\
Z_5 &= g_6\sqrt{x_1}\left(J_0 + x_2\left(J_2 + J_4 x_2\right)\right)\left(x_1 - x_3\right)\sqrt{x_3} \\
Z_6 &= g_6\sqrt{x_1}\sqrt{x_2}\left(-x_1 + x_2\right)\left(J_0 + x_3\left(J_2 + J_4 x_3\right)\right) \\
Z_7 &= -g_6\left(R_0 + x_1\left(R_2 + R_4 x_1\right)\right)\sqrt{x_2}\left(x_2 - x_3\right)\sqrt{x_3} \\
Z_8 &= g_6\sqrt{x_1}\left(R_0 + x_2\left(R_2 + R_4 x_2\right)\right)\left(x_1 - x_3\right)\sqrt{x_3} \\
Z_9 &= g_6\sqrt{x_1}\sqrt{x_2}\left(-x_1 + x_2\right)\left(R_0 + x_3\left(R_2 + R_4 x_3\right)\right)
\end{aligned} \tag{A.1}$$

$$
\begin{aligned}
y_1 =& -d_6d_{12}d_{17}+d_3d_{15}d_{17}+d_7d_{12}d_{17}d_{18}+d_6d_{13}d_{17}d_{18}+d_6d_{14}d_{17}d_{18}-d_4d_{15}d_{17}d_{18}-d_5d_{15}d_{17}d_{18}-d_3d_{16}d_{17}d_{18}-\\
&d_7d_{13}d_{17}d_{18}^2-d_7d_{14}d_{17}d_{18}^2+d_4d_{16}d_{17}d_{18}^2+d_5d_{16}d_{17}d_{18}^2\\
y_2 =& d_6^2d_8-2d_3d_6d_{12}+d_1d_{12}^2+d_3^2d_{15}-d_1d_8d_{15}-d_2d_6^2d_{18}-2d_6d_7d_8d_{18}-d_6^2d_9d_{18}-d_6^2d_{10}d_{18}-d_6^2d_{11}d_{18}+\\
&2d_4d_6d_{12}d_{18}+2d_5d_6d_{12}d_{18}+2d_3d_7d_{12}d_{18}-d_2d_{12}^2d_{18}+2d_3d_6d_{13}d_{18}-2d_1d_{12}d_{13}d_{18}+2d_3d_6d_{14}d_{18}-2d_1d_{12}d_{14}d_{18}+\\
&d_1d_2d_{15}d_{18}-2d_3d_4d_{15}d_{18}-2d_3d_5d_{15}d_{18}+d_2d_8d_{15}d_{18}+d_1d_9d_{15}d_{18}+d_1d_{10}d_{15}d_{18}+d_1d_{11}d_{15}d_{18}-d_3^2d_{16}d_{18}+\\
&d_1d_8d_{16}d_{18}+2d_2d_6d_7d_{18}^2+d_7^2d_8d_{18}^2+2d_6d_7d_9d_{18}^2+2d_6d_7d_{10}d_{18}^2+2d_6d_7d_{11}d_{18}^2-2d_4d_7d_{12}d_{18}^2-2d_5d_7d_{12}d_{18}^2-\\
&2d_4d_6d_{13}d_{18}^2-2d_5d_6d_{13}d_{18}^2-2d_3d_7d_{13}d_{18}^2+2d_2d_{12}d_{13}d_{18}^2+d_1d_{13}^2d_{18}^2-2d_4d_6d_{14}d_{18}^2-2d_5d_6d_{14}d_{18}^2-2d_3d_7d_{14}d_{18}^2+\\
&2d_2d_{12}d_{14}d_{18}^2+2d_1d_{13}d_{14}d_{18}^2+d_1d_{14}^2d_{18}^2-d_2^2d_{15}d_{18}^2+d_4^2d_{15}d_{18}^2+2d_4d_5d_{15}d_{18}^2+d_5^2d_{15}d_{18}^2-d_2d_9d_{15}d_{18}^2-d_2d_{10}d_{15}d_{18}^2-\\
&d_2d_{11}d_{15}d_{18}^2-d_1d_2d_{16}d_{18}^2+2d_3d_4d_{16}d_{18}^2+2d_3d_5d_{16}d_{18}^2-d_2d_8d_{16}d_{18}^2-d_1d_9d_{16}d_{18}^2-d_1d_{10}d_{16}d_{18}^2-d_1d_{11}d_{16}d_{18}^2-\\
&d_2d_7^2d_{18}^3-d_7^2d_9d_{18}^3-d_7^2d_{10}d_{18}^3-d_7^2d_{11}d_{18}^3+2d_4d_7d_{13}d_{18}^3+2d_5d_7d_{13}d_{18}^3-d_2d_{13}^2d_{18}^3+2d_4d_7d_{14}d_{18}^3+2d_5d_7d_{14}d_{18}^3-\\
&2d_2d_{13}d_{14}d_{18}^3-d_2d_{14}^2d_{18}^3+d_2^2d_{16}d_{18}^3-d_4^2d_{16}d_{18}^3-2d_4d_5d_{16}d_{18}^3-d_5^2d_{16}d_{18}^3+d_2d_9d_{16}d_{18}^3+d_2d_{10}d_{16}d_{18}^3+d_2d_{11}d_{16}d_{18}^3\\
y_3 =& -d_6d_{12}d_{19}+d_3d_{15}d_{19}+d_7d_{12}d_{19}d_{20}+d_6d_{13}d_{19}d_{20}+d_6d_{14}d_{19}d_{20}-d_4d_{15}d_{19}d_{20}-d_5d_{15}d_{19}d_{20}-d_3d_{16}d_{19}d_{20}-\\
&d_7d_{13}d_{19}d_{20}^2-d_7d_{14}d_{19}d_{20}^2+d_4d_{16}d_{19}d_{20}^2+d_5d_{16}d_{19}d_{20}^2\\
y_4 =& d_6^2d_8-2d_3d_6d_{12}+d_1d_{12}^2+d_3^2d_{15}-d_1d_8d_{15}-d_2d_6^2d_{20}-2d_6d_7d_8d_{20}-d_6^2d_9d_{20}-d_6^2d_{10}d_{20}-d_6^2d_{11}d_{20}+\\
&2d_4d_6d_{12}d_{20}+2d_5d_6d_{12}d_{20}+2d_3d_7d_{12}d_{20}-d_2d_{12}^2d_{20}+2d_3d_6d_{13}d_{20}-2d_1d_{12}d_{13}d_{20}+2d_3d_6d_{14}d_{20}-\\
&2d_1d_{12}d_{14}d_{20}+d_1d_2d_{15}d_{20}-2d_3d_4d_{15}d_{20}-2d_3d_5d_{15}d_{20}+d_2d_8d_{15}d_{20}+d_1d_9d_{15}d_{20}+d_1d_{10}d_{15}d_{20}+d_1d_{11}d_{15}d_{20}-\\
&d_3^2d_{16}d_{20}+d_1d_8d_{16}d_{20}+2d_2d_6d_7d_{20}^2+d_7^2d_8d_{20}^2+2d_6d_7d_9d_{20}^2+2d_6d_7d_{10}d_{20}^2+2d_6d_7d_{11}d_{20}^2-2d_4d_7d_{12}d_{20}^2-\\
&2d_5d_7d_{12}d_{20}^2-2d_4d_6d_{13}d_{20}^2-2d_5d_6d_{13}d_{20}^2-2d_3d_7d_{13}d_{20}^2+2d_2d_{12}d_{13}d_{20}^2+d_1d_{13}^2d_{20}^2-2d_4d_6d_{14}d_{20}^2-\\
&2d_5d_6d_{14}d_{20}^2-2d_3d_7d_{14}d_{20}^2+2d_2d_{12}d_{14}d_{20}^2+2d_1d_{13}d_{14}d_{20}^2+d_1d_{14}^2d_{20}^2-d_2^2d_{15}d_{20}^2+d_4^2d_{15}d_{20}^2+2d_4d_5d_{15}d_{20}^2+\\
&d_5^2d_{15}d_{20}^2-d_2d_9d_{15}d_{20}^2-d_2d_{10}d_{15}d_{20}^2-d_2d_{11}d_{15}d_{20}^2-d_1d_2d_{16}d_{20}^2+2d_3d_4d_{16}d_{20}^2+2d_3d_5d_{16}d_{20}^2-d_2d_8d_{16}d_{20}^2-\\
&d_1d_9d_{16}d_{20}^2-d_1d_{10}d_{16}d_{20}^2-d_1d_{11}d_{16}d_{20}^2-d_2d_7^2d_{20}^3-d_7^2d_9d_{20}^3-d_7^2d_{10}d_{20}^3-d_7^2d_{11}d_{20}^3+2d_4d_7d_{13}d_{20}^3+2d_5d_7d_{13}d_{20}^3-\\
&d_2d_{13}^2d_{20}^3+2d_4d_7d_{14}d_{20}^3+2d_5d_7d_{14}d_{20}^3-2d_2d_{13}d_{14}d_{20}^3-d_2d_{14}^2d_{20}^3+d_2^2d_{16}d_{20}^3-d_4^2d_{16}d_{20}^3-2d_4d_5d_{16}d_{20}^3-\\
&d_5^2d_{16}d_{20}^3+d_2d_9d_{16}d_{20}^3+d_2d_{10}d_{16}d_{20}^3+d_2d_{11}d_{16}d_{20}^3
\end{aligned}
\tag{A.2}
$$

$$
\begin{aligned}
g_0 =& d_6^2d_8-2d_3d_6d_{12}+d_1d_{12}^2+d_3^2d_{15}-d_1d_8d_{15}\\
g_2 =& d_2d_6^2+2d_6d_7d_8+d_6^2d_9+d_6^2d_{10}+d_6^2d_{11}-2d_4d_6d_{12}-2d_5d_6d_{12}-2d_3d_7d_{12}+d_2d_{12}^2-2d_3d_6d_{13}+2d_1d_{12}d_{13}-\\
&2d_3d_6d_{14}+2d_1d_{12}d_{14}-d_1d_2d_{15}+2d_3d_4d_{15}+2d_3d_5d_{15}-d_2d_8d_{15}-d_1d_9d_{15}-d_1d_{10}d_{15}-d_1d_{11}d_{15}+d_3^2d_{16}-d_1d_8d_{16}\\
g_4 =& 2d_2d_6d_7+d_7^2d_8+2d_6d_7d_9+2d_6d_7d_{10}+2d_6d_7d_{11}-2d_4d_7d_{12}-2d_5d_7d_{12}-2d_4d_6d_{13}-2d_5d_6d_{13}-\\
&2d_3d_7d_{13}+2d_2d_{12}d_{13}+d_1d_{13}^2-2d_4d_6d_{14}-2d_5d_6d_{14}-2d_3d_7d_{14}+2d_2d_{12}d_{14}+2d_1d_{13}d_{14}+d_1d_{14}^2-d_2^2d_{15}+d_4^2d_{15}+\\
&2d_4d_5d_{15}+d_5^2d_{15}-d_2d_9d_{15}-d_2d_{10}d_{15}-d_2d_{11}d_{15}-d_1d_2d_{16}+2d_3d_4d_{16}+2d_3d_5d_{16}-d_2d_8d_{16}-d_1d_9d_{16}-d_1d_{10}d_{16}-d_1d_{11}d_{16}\\
g_6 =& d_2d_7^2+d_7^2d_9+d_7^2d_{10}+d_7^2d_{11}-2d_4d_7d_{13}-2d_5d_7d_{13}+d_2d_{13}^2-2d_4d_7d_{14}-2d_5d_7d_{14}+2d_2d_{13}d_{14}+d_2d_{14}^2-\\
&d_2^2d_{16}+d_4^2d_{16}+2d_4d_5d_{16}+d_5^2d_{16}-d_2d_9d_{16}-d_2d_{10}d_{16}-d_2d_{11}d_{16}
\end{aligned}
\tag{A.3}
$$

$$f_0=\frac{-d_6d_{12}d_{17}+d_3d_{15}d_{17}}{d_{18}}-\frac{r_1y_1}{d_{18}y_2}+\frac{-d_6d_{12}d_{19}+d_3d_{15}d_{19}}{d_{20}}-\frac{r_1y_3}{d_{20}y_4}+$$
$$r_1=d_6^2d_8-2d_3d_6d_{12}+d_1d_{12}^2+d_3^2d_{15}-d_1d_8d_{15}$$
$$f_4=-\frac{r_2y_1}{y_2}-\frac{r_2y_3}{y_4}$$
$$r_2=d_2d_7^2+d_7^2d_9+d_7^2d_{10}+d_7^2d_{11}-2d_4d_7d_{13}-2d_5d_7d_{13}+d_2d_{13}^2-2d_4d_7d_{14}-2d_5d_7d_{14}+2d_2d_{13}d_{14}+d_2d_{14}^2-$$
$$d_2^2d_{16}+d_4^2d_{16}+2d_4d_5d_{16}+d_5^2d_{16}-d_2d_9d_{16}-d_2d_{10}d_{16}-d_2d_{11}d_{16} \tag{A.4}$$
$$f_2=-\frac{y_1}{d_{18}^2}-\frac{y_1r_3}{d_{18}^2y_2}-\frac{y_3}{d_{20}^2}-\frac{y_3r_3}{d_{20}^2y_4}$$
$$r_3=-d_6^2d_8+2d_3d_6d_{12}-d_1d_{12}^2-d_3^2d_{15}+d_1d_8d_{15}+d_2d_6^2d_{18}+2d_6d_7d_8d_{18}+d_6^2d_9d_{18}+d_6^2d_{10}d_{18}+d_6^2d_{11}d_{18}-$$
$$2d_4d_6d_{12}d_{18}-2d_5d_6d_{12}d_{18}-2d_3d_7d_{12}d_{18}+d_2d_{12}^2d_{18}-2d_3d_6d_{13}d_{18}+2d_1d_{12}d_{13}d_{18}-2d_3d_6d_{14}d_{18}+2d_1d_{12}d_{14}d_{18}-$$
$$d_1d_2d_{15}d_{18}+2d_3d_4d_{15}d_{18}+2d_3d_5d_{15}d_{18}-d_2d_8d_{15}d_{18}-d_1d_9d_{15}d_{18}-d_1d_{10}d_{15}d_{18}-d_1d_{11}d_{15}d_{18}+d_3^2d_{16}d_{18}-d_1d_8d_{16}d_{18}$$

$$y_5=d_6^2d_{17}-d_1d_{15}d_{17}-2d_6d_7d_{17}d_{18}+d_2d_{15}d_{17}d_{18}+d_1d_{16}d_{17}d_{18}+d_7^2d_{17}d_{18}^2-d_2d_{16}d_{17}d_{18}^2$$
$$y_6=d_6^2d_{19}-d_1d_{15}d_{19}-2d_6d_7d_{19}d_{20}+d_2d_{15}d_{19}d_{20}+d_1d_{16}d_{19}d_{20}+d_7^2d_{19}d_{20}^2-d_2d_{16}d_{19}d_{20}^2$$
$$J_0=\frac{d_6^2d_{17}-d_1d_{15}d_{17}}{d_{18}}-\frac{r_1y_7}{d_{18}y_2}+\frac{d_6^2d_{19}-d_1d_{15}d_{19}}{d_{20}}-\frac{r_1y_8}{d_{20}y_4}$$
$$J_2=\frac{-d_6^2d_{17}+d_1d_{15}d_{17}+2d_6d_7d_{17}d_{18}-d_2d_{15}d_{17}d_{18}-d_1d_{16}d_{17}d_{18}}{d_{18}^2}-\frac{r_3y_5}{d_{18}^2y_2}+$$
$$\frac{-d_6^2d_{19}+d_1d_{15}d_{19}+2d_6d_7d_{19}d_{20}-d_2d_{15}d_{19}d_{20}-d_1d_{16}d_{19}d_{20}}{d_{20}^2}-\frac{r_4y_6}{d_{20}^2y_4}+ \tag{A.5}$$
$$r_4=-d_6^2d_8+2d_3d_6d_{12}-d_1d_{12}^2-d_3^2d_{15}+d_1d_8d_{15}+d_2d_6^2d_{20}+2d_6d_7d_8d_{20}+d_6^2d_9d_{20}+d_6^2d_{10}d_{20}+d_6^2d_{11}d_{20}-$$
$$2d_4d_6d_{12}d_{20}-2d_5d_6d_{12}d_{20}-2d_3d_7d_{12}d_{20}+d_2d_{12}^2d_{20}-2d_3d_6d_{13}d_{20}+2d_1d_{12}d_{13}d_{20}-2d_3d_6d_{14}d_{20}+2d_1d_{12}d_{14}d_{20}-$$
$$d_1d_2d_{15}d_{20}+2d_3d_4d_{15}d_{20}+2d_3d_5d_{15}d_{20}-d_2d_8d_{15}d_{20}-d_1d_9d_{15}d_{20}-d_1d_{10}d_{15}d_{20}-d_1d_{11}d_{15}d_{20}+d_3^2d_{16}d_{20}-d_1d_8d_{16}d_{20}$$
$$J_4=-\frac{r_2y_7}{y_2}-\frac{r_2y_8}{y_4}$$

$$y_7=-d_3d_6d_{17}+d_1d_{12}d_{17}+d_4d_6d_{17}d_{18}+d_5d_6d_{17}d_{18}+d_3d_7d_{17}d_{18}-d_2d_{12}d_{17}d_{18}-d_1d_{13}d_{17}d_{18}-d_1d_{14}d_{17}d_{18}-$$
$$d_4d_7d_{17}d_{18}^2-d_5d_7d_{17}d_{18}^2+d_2d_{13}d_{17}d_{18}^2+d_2d_{14}d_{17}d_{18}^2$$
$$y_8=-d_3d_6d_{19}+d_1d_{12}d_{19}+d_4d_6d_{19}d_{20}+d_5d_6d_{19}d_{20}+d_3d_7d_{19}d_{20}-d_2d_{12}d_{19}d_{20}-d_1d_{13}d_{19}d_{20}-d_1d_{14}d_{19}d_{20}-$$
$$d_4d_7d_{19}d_{20}^2-d_5d_7d_{19}d_{20}^2+d_2d_{13}d_{19}d_{20}^2+d_2d_{14}d_{19}d_{20}^2$$
$$R_0=\frac{-d_3d_6d_{17}+d_1d_{12}d_{17}}{d_{18}}-\frac{r_1y_7}{d_{18}y_2}+\frac{-d_3d_6d_{19}+d_1d_{12}d_{19}}{d_{20}}-\frac{r_1y_8}{d_{20}y_4} \tag{A.6}$$
$$R_2=\frac{d_3d_6d_{17}-d_1d_{12}d_{17}-d_4d_6d_{17}d_{18}-d_5d_6d_{17}d_{18}-d_3d_7d_{17}d_{18}+d_2d_{12}d_{17}d_{18}+d_1d_{13}d_{17}d_{18}+d_1d_{14}d_{17}d_{18}}{d_{18}^2}-\frac{r_3y_7}{d_{18}^2y_2}+$$
$$\frac{d_3d_6d_{19}-d_1d_{12}d_{19}-d_4d_6d_{19}d_{20}-d_5d_6d_{19}d_{20}-d_3d_7d_{19}d_{20}+d_2d_{12}d_{19}d_{20}+d_1d_{13}d_{19}d_{20}+d_1d_{14}d_{19}d_{20}}{d_{20}^2}-\frac{r_4y_8}{d_{20}^2y_4}+$$
$$R_4=-\frac{r_2y_7}{y_2}-\frac{r_2y_8}{y_4}$$

$$
\begin{aligned}
&d_1 = -A_{11}\alpha^2,\ d_2 = -I_0,\ d_3 = B_{11}\alpha^3 - C_{11}\alpha^3,\ d_4 = I_1\alpha,\ d_5 = -I_3\alpha,\ d_6 = C_{11}\alpha^2,\\
&d_7 = I_3,\ d_8 = -2E_{11}\alpha^4 - H_{11}\alpha^4 - D_{11}\alpha^4 + A_{55}\alpha^2 + k_w + k_s\alpha^2 - N_{x0}\alpha^2,\\
&d_9 = I_0 - I_2\alpha^2,\ d_{10} = 2I_4\alpha^2, d_{11} = -I_5\alpha^2,\ d_{12} = H_{11}\alpha^3 - E_{11}\alpha^3 - A_{55}\alpha,\\
&d_{13} = -I_4\alpha,\ d_{14} = I_5\alpha, d_{15} = -H_{11}\alpha^2 + A_{55},\ d_{16} = -I_5, d_{17} = 2P_1\,\alpha V_1\ , d_{18} = \alpha V_1,\\
&d_{19} = 2P_2\,\alpha V_2,\ d_{20} = \alpha V_2
\end{aligned}
\tag{A.7}
$$

REFERENCES

[1] J.R. Vinson, Sandwich Structures, (2001).
[2] C. Wang, J.N. Reddy, K. Lee, Shear deformable beams and plates: Relationships with classical solutions, Elsevier,(2000).
[3] M. Levinson, A new rectangular beam theory, Journal of Sound and vibration, 74(1), 81-87 (1981).
[4] P. Heyliger, J. Reddy, A higher order beam finite element for bending and vibration problems, Journal of Sound and Vibration, 126(2), 309-326 (1988).
[5] S. Marur, T. Kant, Free vibration analysis of fiber reinforced composite beams using higher order theories and finite element modelling, Journal of Sound and Vibration, 194(3), 337-351 (1996).
[6] H. Matsunaga, Vibration and buckling of multilayered composite beams according to higher order deformation theories, Journal of Sound and Vibration, 246(1), 47-62 (2001).
[7] W. Zhen, C. Wanji, An assessment of several displacement-based theories for the vibration and stability analysis of laminated composite and sandwich beams, Composite Structures, 84(4), 337-349 (2008).
[8] S. Kapuria, P. Dumir, N. Jain, Assessment of zigzag theory for static loading, buckling, free and forced response of composite and sandwich beams, Composite Structures, 64(3-4),317-327 (2004).
[9] R. Moreira, J.D. Rodrigues, Static and dynamic analysis of soft core sandwich panels with through-thickness deformation,Composite Structures, 92(2), 201-215 (2010).
[10] P. Vidal, O. Polit, Vibration of multilayered beams using sinus finite elements with transverse normal stress, Composite Structures, 92(6), 1524-1534 (2010).
[11] S. Khalili, Free vibration analysis of sandwich beams using improved dynamic stiffness method, Composite Structures, 92(2), 387-394 (2010).
[12] C. Hwu, W. Chang, H. Gai, Vibration suppression of composite sandwich beams, Journal of Sound and Vibration, 272(1-2), 1-20 (2004).
[13] J. Lou, L. Ma, L.-Z. Wu, Free vibration analysis of simply supported sandwich beams with lattice truss core, Materials Science and Engineering: B, 177(19), 1712-1716 (2012).
[14] E. Piollet, High damping and nonlinear vibration of sandwich beams with entangled cross-linked fibres as core material, Composites Part B: Engineering, 168, 353-366 (2019).
[15] Z. Huang, A finite element model for the vibration analysis of sandwich beam with frequency-dependent viscoelastic material core, Materials, 12(20), 3390 (2019).
[16] M.R.Rokn-Abadi, P. Shahali, H. Haddadpour, Effects of magnetoelastic loads on free vibration characteristics of the magnetorheological-based sandwich beam, Journal of Intelligent Material Systems and Structures, 31(7), 1015-1028 (2020).
[17] F. de Souza Eloy, A numerical-experimental dynamic analysis of composite sandwich beam with magnetorheological elastomer honeycomb core, Composite Structures, 209, 242-257(2019).
[18] Y.Q. Wang, H.L. Zhao, Free vibration analysis of metal foam core sandwich beams on elastic foundation using Chebyshev collocation method, Archive of Applied Mechanics, 89(11), 2335-2349 (2019).
[19] M. Fadaee, Exact solution for shear deformable model of free damped vibration of magnetorheological fluid sandwich beam, Mechanics Based Design of Structures and Machines, 47(5), 568-582 (2019).
[20] Z.-X. Wang, H.-S. Shen, Nonlinear vibration of sandwich plates with FG-GRC face sheets in thermal environments, Composite Structures, 192, 642-653 (2018).
[21] Q. Jin, On static and dynamic snap-throughs of the imperfect post-buckled FG-GRC sandwich beams, Journal of Sound and Vibration, 489, 115684 (2020).
[22] T.D Singha, Free vibration of rotating pretwisted FG-GRC sandwich conical shells in thermal environment using HSDT, Composite Structures, 257, 113144 (2021).
[23] H.-S. Shen, Y. Xiang, Y. Fan, Nonlinear vibration of thermally postbuckled FG-GRC laminated beams resting on elastic foundations, International Journal of Structural Stability and Dynamics, 19(06),1950051 (2019).
[24] H. Mohammadi, M.S. Nematollahi, Improved dynamical response of functionally graded GPL-reinforced sandwich beams subjected to external excitation via nonlinear dispersion pattern, Engineering with Computers, 2021, 1-13 (2021).
[25] S. Amir, Z. Soleimani□Javid, E. Arshid, Size□dependent free vibration of sandwich micro beam with porous core subjected to thermal load based on SSDBT, ZAMM□Journal of Applied Mathematics and Mechanics/Zeitschrift für Angewandte Mathematik und Mechanik, 99(9), e201800334 (2019).
[26] Y. Zhu, Mass production and industrial applications of graphene materials, National Science Review, 5(1), 90-101 (2017).

[27] J. Mao, W. Zhang, H. Lu, Static and dynamic analyses of graphene-reinforced aluminium-based composite plate in thermal environment, Aerospace Science and Technology, 107, 106354 (2020).
[28] J. Mantari, E. Bonilla, C.G. Soares, A new tangential-exponential higher order shear deformation theory for advanced composite plates, Composites Part B: Engineering, 60, 319-328 (2014).
[29] S. Hosseini, O. Rahmani, Exact solution for axial and transverse dynamic response of functionally graded nanobeam under moving constant load based on nonlocal elasticity theory, Meccanica, 52(6), 1441-1457 (2017).
[30] H. Wu, S. Kitipornchai, J. Yang, Free vibration and buckling analysis of sandwich beams with functionally graded carbon nanotube-reinforced composite face sheets, International Journal of Structural Stability and Dynamics, 15(07), 1540011 (2015).
[31] M. Eghbali, S.A. Hosseini, O. Rahmani, Free vibration of axially functionally graded nanobeam with an attached mass based on nonlocal strain gradient theory via new ADM numerical method, Amirkabir Journal of Mechanical Engineering, 53(2), 8-8 (2021).
[32] A. Khdeir, O. Aldraihem, Free vibration of sandwich beams with soft core, Composite Structures, 154, 179-189 (2016).